Elsevier Editorial System(tm) for Journal of Proteomics
Manuscript Draft

Manuscript Number: JPROT-D-12-00336R1

Title: UNDERSTANDING THE MECHANISMS OF CHILLING INJURY IN BELL PEPPER FRUITS USING THE PROTEOMIC APPROACH

Article Type: Original Article

Keywords: Carbohydrate metabolism; Capsicum annuum; Cold stress; Proteome; cell ultrastructure; 2D-DIGE.

Corresponding Author: Mrs Paloma Sanchez-Bel, Ph.D

Corresponding Author's Institution: CEBAS-CSIC

First Author: Paloma Sanchez-Bel, Ph.D

Order of Authors: Paloma Sanchez-Bel, Ph.D; Isabel Egea, Ph.D; Maria Teresa Sanchez-Ballesta, Ph.D; Concepcion Martinez-Madrid, Ph.D; Nieves Fernandez-Garcia, Ph.D; Felix Romojaro, Professor; Enrique Olmos, Ph.D; Emilio Estrella, Ph.D; Maria C Bolarin, Professor; Francisco Borja Flores, Ph.D

Abstract: In order to advance in the understanding of CI in pepper fruits, the cell ultrastructure alterations induced by CI and the physiological and metabolic changes have been studied along with the proteomic study. When stored at low temperatures bell pepper (Capsicum annuum) fruits exhibited visual CI symptoms and important alterations within the cell ultrastructure, since peroxisomes and starch grains were not detected and the structure of the chloroplast was seriously damaged in chilled tissues. Physiological and metabolic disorders were also observed in chilled fruits, such as higher ethylene production, increased MDA content, changes in sugar and organic acids and enzymatic activities. The comparative proteomic analysis between control and chilled fruits reveals that the main alterations induced by CI in bell pepper fruits are linked to redox homeostasis and carbohydrate metabolism. Thus, protein abundance in the ascorbate-glutathione cycle is altered and catalase is down-regulated. Key proteins from glycolysis, Calvin cycle and Krebs cycle are also inhibited in chilled fruits. Enolase and GAPDH are revealed as proteins that may play a key role in the development of chilling injury. This study also provides the first evidence at the protein level that cytosolic MDH is involved in abiotic stress.

*Graphical Abstract (for review)

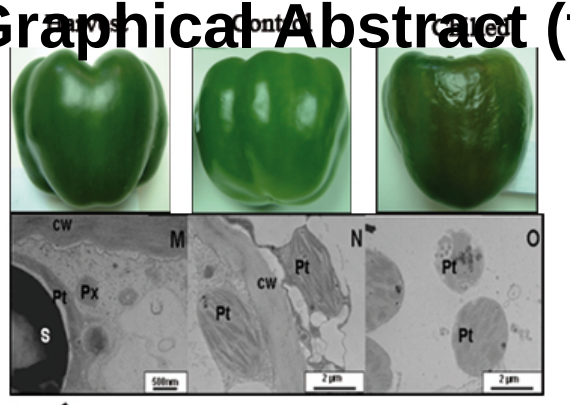

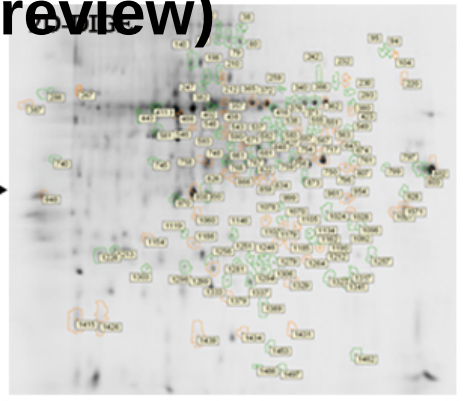

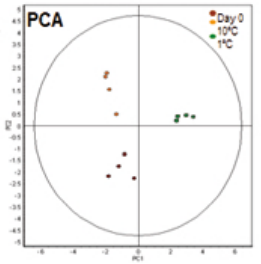

Physiological parameters & metabolite content

	Control	Chilled
Ethylene (nL g^{-1} h^{-1})	0.75 ± 0.015 a	5.07 ± 1.15 b
Lipid peroxidation (nmol MDA g^{-1} h^{-1})	99.45 ± 3.80 a	117.20 ± 3.01 b
Sucrose (mg 100g FW^{-1})	0.16 ± 0.01 a	0.32 ± 0.03 b
Glucose (mg 100g FW^{-1})	2.42 ± 0.25 a	2.13 ± 0.17 a
Fructose (mg 100g FW^{-1})	2.28 ± 0.13 a	2.82 ± 0.24 b
Oxalic acid (mg 100g FW^{-1})	2.86 ± 0.22 b	1.95 ± 0.23 a
Citric acid (mg 100g FW^{-1})	2.90 ± 0.15 b	1.26 ± 0.17 a
Malic acid (mg 100g FW^{-1})	nd	1.73 ± 0.67
Succinic acid (mg 100g FW^{-1})	7.02 ± 1.07 a	9.66 ± 4.69 b
Ascorbic acid (mg 100g FW^{-1})	196.11 ± 11.82 b	120.55 ± 2.73 a

Ascorbate cycle

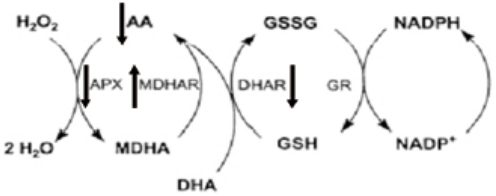

Redox metabolism

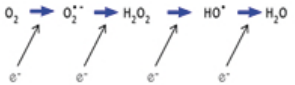

Carbohydrate metabolism

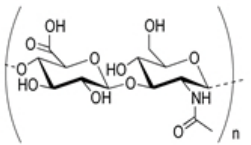

***Highlights (for review)**

- The proteome profile of chilled bell pepper fruits was determined.
- Microscopic, physiological and metabolic changes induced by CI were studied.
- The main alterations are linked to redox homeostasis and carbohydrate metabolism.
- Enolase and GAPDH are revealed as possible key proteins in the CI development.
- First evidence at protein level is provided that cyMDH is involved in abiotic stress.

UNDERSTANDING THE MECHANISMS OF CHILLING INJURY IN BELL PEPPER FRUITS USING THE PROTEOMIC APPROACH

Paloma Sánchez-Bel[1*], Isabel Egea[1], María Teresa Sánchez-Ballesta[2], Concepción Martinez-Madrid[3], Nieves Fernandez-Garcia[1], Félix Romojaro[1], Enrique Olmos[1], Emilio Estrella[4], Maria C Bolarín[1], Francisco Borja Flores[1].

RUNNING TITLE: Proteomics of chilling injury in bell pepper fruits

[1] Centro de Edafología y Biología Aplicada del Segura, Consejo Superior de Investigaciones Científicas (CEBAS-CSIC), Campus de Espinardo, P.O. Box 164, E-30100 Espinardo-Murcia, Spain.

[2] Instituto de Ciencia y Tecnología de Alimentos y Nutrición, Consejo Superior de Investigaciones Científicas (ICTAN-CSIC), C/ Jose Antonio Novais 10, 28040 Madrid, Spain

[3] Escuela Politécnica Superior de Orihuela, Universidad Miguel Hernández (EPSO-UMH), Ctra. Beniel km 3.2, 03312-Orihuela, Alicante, Spain

[4] Dpto Ingenieria Civil, Univ. Politécnica de Cartagena. Pza Cronista Isidoro Valverde, CP 30202. Cartagena-Murcia, Spain.

***Corresponding author:** Paloma Sanchez-Bel

Department of Biology of stress and plant pathology

CEBAS-CSIC. P.O. Box 164, E-30100 Espinardo-Murcia, Spain.

Tel: +34 968396220

Fax: +34 968396213

E-mail: palomasb@cebas.csic.es

ABSTRACT

In order to advance in the understanding of CI in pepper fruits, the cell ultrastructure alterations induced by CI and the physiological and metabolic changes have been studied along with the proteomic study. When stored at low temperatures bell pepper (*Capsicum annuum*) fruits exhibited visual CI symptoms and important alterations within the cell ultrastructure, since peroxisomes and starch grains were not detected and the structure of the chloroplast was seriously damaged in chilled tissues. Physiological and metabolic disorders were also observed in chilled fruits, such as higher ethylene production, increased MDA content, changes in sugar and organic acids and enzymatic activities. The comparative proteomic analysis between control and chilled fruits reveals that the main alterations induced by CI in bell pepper fruits are linked to redox homeostasis and carbohydrate metabolism. Thus, protein abundance in the ascorbate-glutathione cycle is altered and catalase is down-regulated. Key proteins from glycolysis, Calvin cycle and Krebs cycle are also inhibited in chilled fruits. Enolase and GAPDH are revealed as proteins that may play a key role in the development of chilling injury. This study also provides the first evidence at the protein level that cytosolic MDH is involved in abiotic stress.

Keywords: Carbohydrate metabolism; *Capsicum annuum*; Cold stress; Proteome; cell ultrastructure; 2D-DIGE.

INTRODUCTION

In addition to its economic importance, consumption of sweet cultivars of *Capsicum annuum* has been demonstrated to be beneficial to human health [1]. To maintain fruit quality and to avoid fruit decay, bell peppers must be cooled as rapidly as possible, at least to7.5 ºC [2]. However, the ability to prolong the postharvest life of this non-climacteric fruit by storing it at low temperatures is compromised, since the species is sensitive to chilling injury (CI) when stored at temperatures lower than 7 ºC [3]. Visual CI symptoms include surface pitting, seed browning, tissue discoloration, shrivelling resulting from moisture loss, and depressions in the pericarp that evolve into scalds at advanced stages of the physiopathy.

Physiological events related to CI have been extensively described [4]. Modifications in membranes composition and especially in the saturation degree of their constitutive lipids, which regulate membrane fluidity and permeability, are the first notable effects of CI [5]. An exacerbation of oxidative stress due to the overproduction of reactive oxygen species (ROS) has been considered a secondary effect of CI [6, 7]. However, the molecular bases of low temperature stress, that is, perception, signal transduction and finally gene and protein expression changes induced by this environmental factor have been scarcely studied [8]. To our knowledge, only one comprehensive transcriptomics study has been carried out on hot pepper plants subjected to cold stress [9], although no study has been carried out until now on pepper fruit stored at low temperatures. Although gene expression is a highly regulated process, its determination as existing levels of mRNA does not, finally, allow the accurate prediction of expression or activity of the final gene product, in most cases a protein [10]. Alterations in gene expression as a result of stressful conditions often result in modifications of protein concentrations, but this relationship is not always straightforward or linear.

The potentialities and the development of proteomics in recent years have triggered a scientific burst in all biological sciences and, consequently, fruit proteomics is now a corpus of knowledge and of interest not only for academia but also for the agro-food industry. Proteomics has been recently applied in studies on the molecular physiology of fruit development and ripening [11]. However, papers about proteomics approaches dealing with CI in fruits have only been published recently, in particular in the last three years., Two climacteric fruits, peach [12, 13, 14, 15] and tomato [16, 17, 18] have been used as fruit models for this type of study. Although some research works and reviews have suggested a possible implication of the climacteric behavior of the fruit in the sensitivity and development of CI [4, 19] analysis of differentially expressed proteins under low temperature stress conditions in non-climacteric fruits has not been approached yet. In this paper a proteomics study of CI in a non-climacteric fruit such as bell pepper has been carried out applying 2D-DIGE coupled with MALDI-TOF-MS.

Furthermore, microscopic analysis has been performed in order to detect cell ultrastructure alterations induced by CI. This analysis together with the physiological and metabolic data, have been fulfilled in order to integrate these results within the proteomic study. The strategy of integrating physiological and metabolic data with those coming from proteomics has allowed us to elucidate at the protein level the mechanisms and metabolisms most affected by CI. The microscopic images have allowed us to visualize the cellular structures affected by cold stress in pepper fruits. This last approach gives us an accurate image of what is occurring during chilling on cell organelles stability, which has a direct effect on the protein profile of those cell compartments.

MATERIALS AND METHODS

Plant material and cold treatment.

Bell pepper fruits (*Capsicum annuum* L. var. 'California') were obtained from a local producer and selection was based on size uniformity, color and absence of defects. They were divided into three groups; each group consisted of four sub-samples (biological replicates) and each sub-sample consisted of three fruits: one group was analyzed on harvest day (H), another group was stored at 1 ºC (chilled samples, Ch) and the last group was stored at 10 ºC (control samples, C), in both cases in darkness. The storage period was 21 days and relative humidity (RH) was maintained at 80% in both samples, Ch and C. After storage, fruits were transferred to a reconditioning chamber at 20 ºC and 80% RH for 72h, also in darkness, before proceeding with the analyses; thus the total storage period was 24 days (21 days at 1 ºC or 10 ºC plus 3 days at 20 ºC). After this reconditioning period, ethylene production was measured. The whole pericarp tissue was collected and frozen in liquid nitrogen, and stored at -70 ºC until lyophilization was fulfilled.

Transmission electron microscopy

Pepper fruit sections were embedded as previously described [20]. Sections (1 × 3 mm) were fixed with 2.5% glutaraldehyde and 4% paraformaldehyde in 0.1 M sodium phosphate buffer (pH 7.2) for 2.5 h. After three 15 min. washes with the buffer, the samples were post-fixed in 1% osmium tetroxide, in the same buffer, for 2 h. After this, three washes with phosphate buffer were performed. All fixed tissues were dehydrated in a graded series of ethanol (35, 50, 70, 96 and 100%), then infiltrated, first with propylene oxide and then with propylene oxide and Spurr's resin mixture. The samples were then immersed in Spurr's resin overnight at 4°C. Finally, the samples were embedded in Spurr resin. Blocks were sectioned on a Leica EM UC6 ultramicrotome, collected on copper grids and stained with uranyl acetate followed by lead citrate. Sections were examined using a Philips Tecnai 12 transmission electron microscope.

Ethylene production.

Ethylene was measured by GC-FID according to Egea et al. [21]. Fruits were placed in jars, hermetically sealed with a rubber stopper. After 1h, 1 mL sample of the internal atmosphere of the jar was extracted and ethylene production was quantified in a Hewlett-Packard gas chromatograph model 5890, equipped with a flame ionization detector and stainless steel column (3 m x 3.25 mm i.d.) containing activated 80/100 mesh alumina. The flow rates of carrier gas (nitrogen), hydrogen and air were 32, 26 and 400 mL min^{-1}, respectively, and the temperatures of the column, injector and detector were 70, 150 and 175 ºC, respectively. The quantification was carried out by calibration, point-by-point, with an external standard. Results were expressed as nL of ethylene produced per gram of fresh weight and hour (nL $g^{-1}h^{-1}$).

Determination of ascorbate content.

Fruit ascorbate (ASC) content was determined according to Egea et al. [21] with slight modifications. Lyophilized tissue (0.1 g) was ground in an ice bath with 10 mL 5% metaphosphoric acid stored at 4 ºC, and then the final mix was homogenized by Vortex. The final solution was maintained on the ice bath, in darkness, for 30 min and then centrifuged at 20,000 × *g* for 25 min at 4 ºC. After centrifugation, the supernatant phase was purified through a C18 column (Sep-pak plus, Waters) and a 0.2 µm filter (Millipore). Analyses were carried out with a HPLC equipment (Shimadzu LC-10Atvp), using a thermostatized ion-exchange column (ION-300, Tecknocroma) at 30 ºC and applying an isocratic elution of the mobile phase (H_2SO_4 5 mM) at a flow rate of 0.35 mL min^{-1}. Ascorbate was spectrophotometrically detected by registering absorbance at 254 nm wavelength by means of a UV detector. For quantification of the compound a calibration curve in the range of 10–100 mg kg^{-1} was prepared from standard ascorbic acid. Results were expressed as mg 100 g^{-1} FW.

Lipid Peroxidation Measurement.

Malonyl-dialdehyde (MDA) production was used as the analytical parameter to determine the index of lipid peroxidation, using the thiobarbituric acid reactive substrates (TBARS) assay to measure it. Extraction and determination of MDA content was performed according to Martinez-Solano et al. [22] with slight modifications: 0.2 g of lyophilized pepper tissue was homogenized in 4 mL of 0.1% trichloroacetic acid (TCA) solution. Results were expressed as nmol MDA produced per gram FW per hour (nmol MDA g^{-1} h^{-1}).

Sugar and Organic Acids Content.

Sugars and organic acids were extracted according to the procedure of Sanchez-Bel et al. [23]. The extract was filtered through a Durapore 0.45 μm HV (Milipore Corporation) membrane disk and then passed through a C18 Plus Sep-Pak cartridge (Waters Corporation, Massachusetts).Quantification was carried out by high-performance liquid chromatography (HPLC; Shimadzu, Kyoto, Japan) using a thermostatized ion-exchange column (ION-300, Teknochroma) at 30 ºC, with isocratic elution of mobile phase made of H_2SO_4 2.5 mM and a flow rate of 0.4mL.min^{-1}, and with two detectors connected in tandem: a Shimadzu Refractive Index Detector (RIL-10Avp, Kyoto, Japan) for detection of sugars, and a Shimadzu UV-Vis Spectrophotometric Detector (UV-10Avo,Kyoto, Japan) for detection of organic acids. The wavelengths for UV detection of organic acids were 210 nm for oxalic acid and 230 nm for citric, malic, and succinic acids. The sugars and organic acids quantifications were performed by means of calibration curves for each compound prepared with solutions made of standards of each organic acid and sugar (Sanchez-Bel et al., 2008). Results of sugars and organic acids are expressed as mg per 100g of fresh weight.

Extraction and analysis of antioxidant enzymes (Supplementary table S1)

Enzymes extractions and analyses (Guaiacol peroxidase, POX; EC 1.11.1.7, and Catalase, CAT; EC 1.11.1.6) were carried out according to Martínez-Solano et al. [22]. Enzyme activities were expressed as specific activities (units per mg protein). Protein concentration was measured using the Bio-Rad DC protein kit.

Statistical analysis of physiological and biochemical data.

Tests for significant differences were carried out using the General Linear Model of the SPSS (version 11.0) statistical package. Analysis of variance (ANOVA) was performed to compare mean values for each variable using the treatments as a statistical parameter, considering a confidence level of 95%. Parameters were analyzed, for the same day of storage, by unpaired Student's t-test at a stringency of $p<0.05$.

Protein extraction and preparation.

Samples at harvest day and those stored during 24 days (21 days at 1 ºC or 10 ºC plus 3 days at 20 ºC) were used for the proteomics analysis. Soluble proteins were extracted by adding 1.5 mL of extraction buffer [50 mM sodium phosphate buffer at pH 7.8 containing 1 mM EDTA, 0.2% Triton X-100, 2% poly(vinylpyrrolidone) (PVP), 1 mM DTT and protease inhibitor (Complete, Roche) to 100 mg lyophilized pericarp powder, followed by 1 min of Vortex agitation. The homogenate was chilled at 4 °C and then a centrifugation step at 18000 × *g* and 4 ºC for 15 min was fulfilled. The supernatant phase was collected and desalted through a Sephadex G-25 (NAP-10, Gealthcare) column. The sample was collected in 50 mM sodium phosphate buffer pH 7.8 and total protein was quantified using the Bio-Rad DC protein assay kit, based on the method described by Lowry et al. [24], using bovine serum albumin as standard to prepare the calibration curve for quantification.

DIGE experimental design.

DIGE experiments and protein identification were performed at the Proteomic Facility of the Universidad Complutense -Parque Científico de Madrid, Spain (UCM-PCM), a member of ProteoRed Network (http://www.ucm.es/info/gyp/proteomica/en/index.htm). Following extraction, interfering components were removed by using 2D-Clean Kit™ (GE Healthcare). The proteins were resuspended in 10 mM Tris buffer pH 8.5 containing 7 M urea, 2 M thiourea and 2% v/w CHAPS. The protein concentration was determined using 2D-Quant Kit™ (GE Healthcare). Each experiment group contained four biological replicates, generating 12 individual samples that were distributed across six DIGE gels with the internal standard pooled sample also present in each separation. The samples were labeled using the CyDye DIGE Fluor minimal dye (GE Healthcare,) following the manufacturer's recommendation for minimal labeling. Four hundred pmol of CyDye in one mL of anhydrous DMF was used per 50 mg of protein for the labeling. After 30 min of incubation on ice in the dark, the reaction was quenched with 10 mM lysine and incubated for 10 min. Samples were combined according to the experimental design and an equal volume of rehydration buffer (7 M urea, 2 M thiourea, 4% w/v CHAPS, 2% v/w DTT and 4% pharmalytes pH 3–11) was added for the cup loading. 2-DE was performed using GE Healthcare reagents and equipment. First dimension IEF was performed on 24-cm 3–11 NL pH range IPG strips, previously rehydrated with 7 M urea, 2 M thiourea, 4% w/v CHAPS, 100 mM DeStreak and 2% pharmalytes pH 3–11. IEF was performed at 20 ºC using the following program: 120 V for 1 h, 500 V for 2 h, 500–2000 V for 2 h, 1000–5000 V for 6 h and 5000 V for 10 h. After this, strips were firstly equilibrated for 12 min in reducing solution (6 M urea, 50 mM Tris-HCl pH 6.8, 30% v/v glycerol, 2% w/v SDS and 2% w/v DTT) and secondly for 5 min in alkylating solution (6 M urea, 50 mM Tris- HCl pH 6.8, 30% v/v glycerol, 2% w/v SDS and 2.5% w/v iodoacetamide). Second dimension SDS-PAGE were run on homogeneous 12% T,

2.6% C (piperazine diacrylamide) polyacrylamide gels cast in low fluorescent glass plates. Electrophoresis was carried out at 20 ºC, 15 W/gel using Ettan-Dalt six unit.

Image acquisition and DIGE analysis.

Proteins were visualized using a Typhoon 9400™ scanner (GE Healthcare) with CyDye filters. For the Cy3, Cy5 and Cy2 image acquisition, the 532 nm/580 nm, 633 nm/670 nm and 488 nm/520 nm excitation/emission wavelengths, respectively, and 100 mm as pixel size were used. Image analysis was carried out with DeCyder™ differential analysis software v 6.5 (GE Healthcare). The DIA module was used to assign spot boundaries and to calculate parameters such as normalized spot volumes. Inter-gel variability was corrected by matching and normalization of the internal standard spot maps in the biological variance analysis (BVA) module. The internal standard image gel with the greatest number of spots was used as a master gel. Three comparisons were carried out: chilled samples versus harvest day; control samples versus harvest day; and chilled versus control samples. Average ratio and unpaired Student's t-test were calculated between groups. In order to reduce the false positive, False Discovery Rate (FDR) was applied. Protein spots with 1.5-fold as threshold in the average ratio with p-values less than 0.05 were considered as differentially expressed with statistical significance between extracts under comparison. Unsupervised multivariate analysis was performed using the extended data analysis (EDA) module. PCA analysis was performed following the nonlinear iterative partial least squares method.

Protein identification.

Total protein profile was detected by staining the DIGE gels with CBB. Proteins selected for analysis were in-gel digested [25]. Samples were reduced with 10 mM DTT in 25 mM ammonium bicarbonate for 30 min at 56 ºC and subsequently alkylated with 55 mM iodoacetamide in 25 mM ammonium bicarbonate for 20 min in the dark.

Finally, samples were digested overnight at 37 ºC with 12.5 ng mL^{-1} sequencing grade trypsin (Roche Molecular Biochemicals) in 25 mM ammonium bicarbonate (pH 8.5). After digestion, the supernatant was collected and 1 mL was spotted onto a MALDI target plate and allowed to air-dry at room temperature. Then, 0.4 mL of a 3 mg/mL of CHCA matrix (Sigma) in 50% v/v ACN was added to the dried peptide digest spots and again allowed to air-dry at room temperature. MALDI-TOF MS analyses were performed in a MALDI-TOF/ TOF mass spectrometer 4700 Proteomics Analyzer (Per-Septives Biosystems, Framingham, MA). The instrument was operated in reflector mode, with an accelerating voltage of 20000 V. All mass spectra were calibrated externally using a standard peptide mixture (Sigma). Peptides from the auto digestion of the trypsin were used for the internal calibration. MALDI-TOF MS analysis produces peptide mass fingerprints and the peptides observed can be collected and represented as a list of monoisotopic molecular weights with an S/N greater than 20. The suitable precursors for MS/MS sequencing analyses were selected and fragmentation was carried out using the CID on (atmospheric gas was used) 1 KV ion reflector mode and precursor mass Windows 610 Da. The plate model and default calibration were optimized for the MS/MS spectra processing. The search for peptides was performed in batch mode using GPS Explorer v3.5 software with a licensed version 1.9 of MASCOT, using viridiplantae database.

Biological processes and functions involving differentially abundant proteins.

The differential abundance of proteins in the three experimental conditions was statistically analysed by ANOVA ($p<0.01$) followed by the Tukey Multiple Comparison Test ($p<0.05$). Proteins description and functional assignments were performed using annotations associated with each protein entry and through homology-based comparisons with the TAIR10 protein database (http://www.arabidopsis.org/), using

Basic Local Alignment Search Tool BLASTX [26] with an e-value cut-off of $1.e^{-5}$ to avoid false positives. Linked Mapman Bins were used for functional assignments (http://mapman.mpimp-golm.mpg.de/).

RESULTS

Development of visual symptoms of chilling injury and effects on cellular ultrastructure.

Both pepper fruits stored under optimal (10 ºC) and CI-inducing (1 ºC) temperatures were reconditioned at 20 ºC during three days, since it is during this rewarming period when CI-affected fruits exhibit visual symptoms caused by the physiopathy. Control fruits do not appear to be affected during the storage period (Figure 1, image A1), whereas chilled fruits were clearly affected by cold stress, exhibiting typical CI symptoms: surface pitting and shrivelling (Figure 1, image A2).

The ultrastructure of pericarp in control and chilled pepper fruits was analysed by transmission electron microscopy. Epidermal cells of chilled pepper fruits showed collapsed cytoplasms in comparison with harvest day and control samples (Figure 1 A, B and C). Similarly, collenchymatic cells (under the epidermal cell layer) were also highly affected by cold storage; cytoplasms of chilled samples were collapsed and degraded in comparison with harvest day and control samples (Figure 1 D, E and F). The pericarp of pepper fruit is mainly composed of mesocarp cells which are bigger in volume than epidermal and collenchymatic cells. These results showed that mesocarp cells of chilled samples were also affected, although it was possible to find some cells showing unaltered ultrastructure (Figure 1 G, H and I). Plastids in harvest day samples showed a different ultrastructure depending on the cell type. Epidermal and collenchymatic cells showed a typical discoidal shape with abundant plastoglobuli (Figure 1 A and J). However, plastids in mesocarp cells showed abundant starch grains

297 and lower amounts of plastoglobuli (Figure 1 G and M). Control samples, showed some
298 altered plastids in collenchymatic and mesocarp cells; these plastids have disrupted
299 grana but the thylakoids are still stacked and show starch grains (Figure 1 K and N).
300 However, chilled samples showed great differences compared with control and harvest
301 day samples. In the majority of epidermal and collenchyma cells, plastids are degraded
302 (Figure 1 L). Plastids of mesocarp cells were also altered (Figure 1 O) but it was
303 possible to observe some cells with unaltered plastids (Figure 1 I). Cells of pepper fruit
304 have abundant peroxisomes in the cytoplasm as can be observed in harvest day sample
305 (Figure 1 M) but also in samples stored at 10ºC. However, in chilled samples the
306 peroxisomes abundance decreased drastically (Figure 1 O).

307 **Physiological and metabolic response of bell pepper fruits to Chilling Injury.**

308 Parallel to the development of CI visual symptoms, chilled fruits showed a significant
309 (p<0.05) rise of ethylene production that did not come up with control fruits (Table 1).
310 One typical feature of CI is the induction of oxidative stress, which it is possible to
311 determine through the rise of lipid peroxidation. In this study, lipid peroxidation of
312 fruits was measured as MDA production and was significantly higher (p<0.05) in
313 chilled samples compared with control fruits (Table 1). Sucrose and fructose contents
314 increased significantly (p<0.05) in chilled fruits compared with control ones, while
315 glucose content was not affected. With regard to organic acids contents, the levels of
316 oxalic and citric acids were significantly (p<0.05) reduced in chilled fruits compared to
317 control ones whilst that of succinic acid seems not to be affected by cold storage. One
318 remarkable feature of this analysis was the malic acid, which was not detected in control
319 and harvest day fruits but did come up in chilled fruits (Table 1). Ascorbate content
320 (ASC) was significantly (p<0.05) reduced in chilled fruits compared to control fruits.

Proteomic analysis of bell pepper fruits subjected to chilling and non-chilling temperature storage.

Representative 2D-DIGE maps of proteins using an optimized extraction procedure are provided as Supporting Information (Figure S1 of supplementary data). A total of 18 2D gel images from 6 2D-DIGE gels corresponding to harvest and the two storage conditions (1 ºC and 10 ºC), with 4 biological replicates per sample have been obtained. The distribution pattern of proteins at harvest, and at the end of the storage period for control and chilled fruits are also provided as Supporting Information (Figure S2 of supplementary data). Of the protein profiles of samples from harvest day and the two storage temperatures, a total of 147 spot proteins exhibited a significant variation in their abundance when a one-way analysis of variance (ANOVA) (p<0.05) and a false discovery rate correction test (FDR, q-value of 0.05) were applied (Figure 2A). The differential data set was also subjected to a principal components analysis (PCA) to investigate inter- and intra-group relationships among the three types of samples (Figure 2B). 82.3 percent of the cumulative variance was represented by the first two principal components in PCA (PC1 52.3% and PC2 30%). There is a clear partition between the three types of samples, each one located in one quadrant of the map created by PC1 and PC2. The first principal component (PC1, x-axis) separates chilled samples (positive area) from harvest day and control ones (negative area) while throughout PC2 (y-axis) there is a clear separation of harvest day samples (negative area) from chilled and control samples which are placed on the positive area of the PC2 axis. These data indicate that 52% of variation corresponds to a regulation of protein abundance due to cold storage.

Of the 147 protein spots which exhibited significant variation in their abundance, 106 were down-regulated and 41 were up-regulated. 67 of these proteins could be excised

from the gels and then identified by mass spectrometry. Of this set of 67 proteins, 15 were up-regulated and 52 were down-regulated (Figure 2C). Most of the spots were identified by peptide mass fingerprint. In the particular cases where the identification by mass fingerprint did not supply conclusive results, a peptide fragmentation strategy was performed and the fragmented peptides were searched for independently (MS/MS) or in combination with the search by mass fingerprint. In some cases, when no identification was found in the databases, even with high-quality spectrums of peptides fragmentation, a *de novo* sequencing was carried out and a search by sequence homology was completed in order to provide a more probable sequence identification.

Of the 67 identified proteins that displayed significant differential abundance, 55 exhibited an abundance fold change value higher than 1.5 when chilled samples were compared with control ones. Of this set of 55 proteins, 10 were up-regulated and 45 were down-regulated (Figure 2C).

Functional classification and abundance patterns of protein spots

The 55 proteins identified as having differential abundances and a fold change value higher than 1.5 when compared chilled samples with control samples (Ch/C) were classified into 16 classes according to the bioinformatics tool for functional classification Mapman (Mapman 3.5.1, http://mapman.gabipd.org). Redox and carbohydrate metabolism, this last one comprising glycolysis-, tricarboxylic acids (TCA)- cycle, Calvin cycle and fermentation-metabolism, were the two major functional classes found in our proteomic study (Figure 3A).

Concerning Redox metabolism, four protein spots were up-regulated in chilled fruits compared to control fruits (Ch/C): monodehydroascorbate reductase (MDHAR, spot 581), glutathione-S-transferase (GST, spot 1279), manganese superoxide dismutase (Mn-SOD, spot 1333) and thioredoxin peroxidase (TXP, spot 1439) (table 2). The rest

371 of the proteins belonging to this category were down-regulated in Ch/C; a probable
372 glutathione-S-transferase (GST, spot 1306), a probable NADP-dependent
373 oxidoreductase (spot 822), ascorbate peroxidase (APX, spot 1154), two GSH-dependent
374 dehydroascorbate reductase (GSH-DHAR, spots 1298 and 1299) and four catalase
375 (CAT, spots 230, 362, 366 and 371).
376 Linked to the carbohydrate metabolism, the spots found with differential protein
377 abundance (down-regulated in chilled fruits compared with control fruits) were
378 aldehyde dehydrogenases (ADH spots 357, 365 and 372), glyceraldehyde-3-phosphate
379 dehydrogenase (GAPDH, spots 557, 750, 754, 756, 767, 768), phosphoglucomutase
380 (PGM, spots 198, 212), glucose-6-phosphate isomerase (GPI, spot 259), enolase (spot
381 409), ribulose-1,5-biphosphate carboxylase/oxygenase (RuBisCO, spot 416) large
382 subunit, fructose-biphosphate aldolase (FruBP, spots 717, 834, 873), transketolase
383 (spots 143, 548), malate dehydrogenase (MDH, spots 748, 758), NADP-isocitrate
384 dehydrogenase (NADP-ICDH, spot 582) and citrate synthase (CS, spot 538). The only
385 up-regulated proteins were the enolase and one of the two transketolases (spot 143)
386 (Figure 3A, right-side zoom).
387 Finally, the rest of functional classes correspond mainly to proteins related to stress,
388 amino acid metabolism, cell wall metabolism, nitrogen metabolism, protein
389 degradation, RNA processing, secondary metabolism, and transport.
390 Six different patterns were created from the whole set of protein data on the basis of
391 similar abundance profiles (Figure 3B). Three of these clusters correspond to up-
392 regulated proteins and the other three to down-regulated proteins in response to cold
393 storage when comparing Ch/C. The first pattern (A) is formed by proteins that showed a
394 pronounced increase during the cold storage (Ch/H) compared with a minor increase
395 accumulation during the storage at 10 ºC (C/H). This behaviour is exemplified by a

NAD-dependent formate dehydrogenase, and two PR proteins. The second pattern (B) is formed by proteins exhibiting an increased accumulation during storage at chilling temperature (Ch/H) but they were down-regulated when the samples were stored at 10 ºC (C/H). This cluster is mainly represented by glycolisis- and redox-related proteins. The third pattern (C) is generated by proteins down-regulated both in control and chilled samples when compared with harvest day samples, but the inhibition rate is lower during cold storage than during storage at 10 ºC, and as a result the comparison of Ch/C showed up-regulation. The only protein of this group is a monodehydroascorbate reductase (MDHAR). The opposite arrangement is presented by proteins included in pattern D. In this pattern there are carbohydrate metabolism- and redox-related proteins. These proteins have a lower degree of abundance during postharvest storage compared with harvest day and this inhibition of the protein abundance was more pronounced when the samples were subjected to cold storage (1 ºC). The largest pattern (E) corresponds to proteins that are up-regulated at non-chilling temperature storage and down-regulated in response to storage at 1 ºC, and even in this last type of conservation the protein abundance is lower than in harvest day samples (Ch/H). This pattern is mainly represented by glycolisis-, redox- and TCA cycle- related proteins. The last pattern (F) corresponds to proteins that are up-regulated in both optimal and CI-inducing storage in comparison with harvest day samples, but the increment of the protein accumulation is lower during cold storage (Ch/H) than during storage at 10 ºC (C/H). In this pattern are cell wall metabolism-, amino acids metabolism, redox-, and TCA cycle-related proteins.

It is interesting to underline the pre-eminence of one or another of the above functional classes within the different patterns in which the proteins have been distributed

according to the differential degree of abundance as a consequence of the different postharvest storage temperature applied to the fruits (Table 2).

DISCUSSION

In spite of the numerous studies on the physiopathy of CI, which causes important damages in fruit quality, scarce advances have been achieved until now, probably because the most studies only analyze the physiological changes induced by CI. In this study, besides the physiological and metabolic changes, the damage induced by CI at the cellular level has been analyzed by electron microscopy analysis. Moreover, this is the first proteomic study in pepper fruits subjected to CI. When fruits were analyzed after storage, chilled fruits showed clear visual symptoms of damage and a deep alteration of the cell ultrastructure (Figure 1), few studies have reported results at the subcellular level concerning the effect of cold stress on the ultrastructure of the cells [27]. Changes in physiological and metabolite contents induced by CI confirmed the development of this physiopathy. Thus, an increase in ethylene production was observed in chilled fruits (Table 1). In many cold-sensitive plant systems, low temperatures stimulate ethylene biosynthesis together with development of CI, and these events have been associated with an increase in the contents of precursors of ethylene biosynthesis or in the activities of enzymes involved in the biosynthetic pathway [28, 29, 30].

During CI loss of redox homeostasis because of a disproportionate increase in ROS production, causing oxidative stress is a distinctive effect of low temperatures in plant organs [4]. Changes in MDA production, which reflect the rise of lipid peroxidation of cell membranes caused by ROS accumulation [29], were also observed in chilled fruits (Table 1). It is interesting to point out that the MDA increase in chilled fruits is associated to plastid degradation and the disappearance of peroxisomes in chilled fruits

445 (Figure 1, L, O), the decrease in the activities of antioxidant enzymes (CAT and POX)
446 (supplementary table S1), and the data obtained from the proteomic study (Table 2) in
447 which "redox metabolism" is one of the two major functional classes affected by cold
448 stress.
449 The decrease in the number of peroxisomes, and even their disappearance at chilling
450 temperature storage, may be due to the oxidative degradation of their lipid membrane,
451 since they are extremely fragile organelles surrounded by a single membrane [31]. Thus,
452 ROS accumulation can oxidize their lipid membranes causing the structural
453 disintegration of the organelles as occurred in pepper fruits subjected to other abiotic
454 stresses like ionization treatments [22]. Since CAT is located inside of the peroxisomes,
455 the disintegration of these organelles could explain the decrease in CAT activity and the
456 down-regulation of CAT protein abundance. The accumulation of lipid hydroperoxides
457 found in chilled fruits along with other ROS could be the cause of the up-regulation of
458 TPX found in chilled fruits [32]. Thioredoxin peroxidase plays an important role in
459 plants under abiotic stress conditions through its involvement in regulating redox
460 homeostasis; it has been suggested that this enzyme achieves this role by catalysing the
461 decomposition of the H_2O_2 that escapes detoxification by other antioxidant enzymes
462 such as catalases and other peroxidases [33].
463 The lower capacity of the chilled fruits to re-establish the cellular homeostasis is mainly
464 associated with both down-regulation of CAT and important alterations of the
465 abundance of proteins involved in the ascorbate-glutathione cycle. In a previous
466 proteomic study on tomato, prior to CI symptoms appearance, we observed that redox
467 metabolism was not affected [18], whereas in this study, in which pepper fruits clearly
468 manifested CI symptoms, it is affected. This suggests that redox metabolism alterarions
469 are a consequence of the damage of CI rather than a defence mechanism against stress.

This assumption is also supported a by other proteomic studies on tomatoes were clear CI symptoms were spotted. The proteome of tomato fruits in these studies presented significant changes in the abundance of proteins involved in oxidative homeostasis [16, 17].

To counteract the increased accumulation of ROS, plant responses include the induction of diverse ROS-scavenging systems(enzymatic and non-enzymatic). Detoxification of hydrogen peroxide is performed mainly through APX enzyme belonging to the ascorbate/glutathione cycle (Figure 4), while MDHAR enzyme catalyzes the regeneration of ASC in the chloroplast at the expense of NADH or NADPH [34]. The diminution of ASC observed in the chilled fruits together with the down-regulation of APX and of DHAR would indicate that the capacity of regeneration of ASC was exceeded because of CI and, as a consequence, the ASC pool was depleted (Figure 4). On the other hand, up-regulation of MDHAR in chilled samples may be a consequence of the low content of ASC. Eltelib et al. [35] suggested that the ASC pool is possibly involved in regulating the mRNA expression and activity of MDHAR, and as a result its activity and expression increase in tissues with low ASC content.

In plants, low temperatures stress is known to have significant effects on carbon metabolism and on carbohydrates contents [4, 8]. Many studies have shown that there is a causal link between the cold-induced modulation of sucrose metabolism and cold tolerance [36]. One of the main consequences of chilling injury in affected tissues is the loss of permeability control of the cell membranes which leads to an ion and water leakage and the subsequent osmotic stress [8]. This process is responsible for dehydration, and it has been proposed that sugars have a role as compatible solutes to protect cells against osmotic stress [37]. Thus, exposure of plants to cold stress frequently leads to the mobilization of carbohydrates and this process may involve the

hydrolysis of starch and other polysaccharides or simply the conversion of sucrose to reducing sugars [8]. In this study, starch grains disappear and sucrose and fructose contents increased in chilled fruits. Moreover, most of the proteins involved in carbohydrate metabolism were down regulated by CI. One of the proteins found to be down-regulated was PGM, which plays a pivotal role in the synthesis and breakdown of glucose controlling the flux through the major metabolic pathways. Although little is known about the role of this protein in the plant response to stress, this is not the first time PGM has been reported as being down-regulated by abiotic stress [38]. The enzyme is thought to be responsible for maintaining the Glc-6-P and Glc-1-P balance. The first compound continues its metabolic pathway through glycolysis, while the second is diverted to the metabolism of starch biosynthesis. This result supports the hypothesis that cells are trying to accumulate reducing sugars in two ways; by mobilization of carbohydrates, which would explain the disappearance of the starch grains on chilled samples (Figure 1) and is consistent with the inhibition of PGM (Table 2), and by the down-regulation of the catabolic pathways of sugars as it seems to indicate the sucrose and fructose contents of the chilled fruits compared to control fruits (Table 1).

Enolase is the only up-regulated protein found in the glycolytic metabolism. In addition to its activity in the glycolytic pathway, it has been proposed that enolase is a positive regulator of cold response, since a gene that codes for this enzyme (X58107) has been identified in a transcriptomics study of Arabidopsis subjected to low temperature treatment as a cold-induced gene [39]. A comparison of the protein profiles regarding carbohydrate metabolism among this study on pepper fruit (supplementary table S2) and analogous studies on other species showed that although carbohydrate metabolism seems to be one of the most affected by this stressful condition, only two proteins

overlap between pepper and other species (peach and tomato) irrespectively of the ripening stage of the fruits and the degree of development of CI: enolase [13, 16] and GAPDH [15, 18]. GAPDH has been localized in the nucleus of Arabidopsis plant cells when cold stress occurred [40]. Moreover, its capacity to bind DNA has been observed [41], specifically in the coding sequence of the plastid NADP-dependent malate dehydrogenase (MDH) gene (At5g58340) [42]. This molecular function has been proposed as part of the signalling pathway which goal is increasing the malate-valve capacity [41]. In this study, cytoplasmic malate dehydrogenase is inhibited in chilled samples (Table 2). While plastid MDH has been extensively studied in abiotic stress, this is the first evidence at the protein level of a cytosolic MDH involved in this type of stress. Yao et al. [43] characterised the role of the apple cytoplasmic MDH gene (*MdcyMDH*) in tolerance to cold stress and observed that the transcripts levels were strongly down-regulated when chilling temperatures were applied, as occurred in this study at the protein level. Those authors found that *MdcyMDH* overexpression enhances cold and salt tolerance. The role of cyMDH in cold tolerance can be exerted by means of either altering metabolic energy (ATP) generation [43] or importing malate produced by cyMDH catalytic activity into mitochondria via malate-OAA shuttle in order to maintain the flux of TCA cycle and the subsequent respiratory flux [44, 45]. In this sense, another protein found to be inhibited in pepper chilled samples was Aspartate aminotransferase (AspAT) (Table 2). This protein catalyzes the transfer of the amino group from aspartate to α-ketoglutarate, yielding oxalacetate and glutamate and the inverse reaction [46]. In plants, AspATs have been reported to play an important role in a number of physiological processes including the participation in the malate/aspartate shuttle [47]. Asp is the precursor for several essential amino acids involved in osmotic regulation and they represent the link between the nitrogen and carbon metabolic

pathways [48]. Indeed, the oxalacetate required to synthesize Asp is produced from malate in the TCA cycle through the activity of malate dehydrogenase, whereas α-ketoglutarate can be synthetized by isocitrate dehydrogenase, and by AspAT during Asp production [49]. In this sense, the fact that we found down-regulated the protein AspAT in chilled fruits is in agreement with the observation that almost all proteins associated with the organic acids and sugar catabolic processes, were down-regulated in chilled fruits. Furthermore, every protein related to organic acids metabolism found in this study (cMDH, NAP-ICDH, CS) codes to enzymes that catalyse critical steps where reducing molecules are generated. Studies on pepper plants [50] showed that under cold stress conditions an increase in NADPH production is needed to undergo cold acclimation and a rise in all NAD-dehydrogenases activities occurs.

Modifications in the abundance of Calvin cycle-related proteins were not observed in the proteomic studies carried out with the chilled fruits of tomato and peach [13, 15, 16, 18], even though biochemical and physiological adaptations of plants to low temperature generally include alterations of gene expression and post-translational modifications of enzymes from the sucrose synthesis pathway and from the Calvin cycle. However, in this study, a differential down-regulation abundance of RuBisCo large subunit has been detected in chilled pepper fruits compared with control fruits. This down-regulation of RuBisCO and other enzymes of Calvin cycle seem to be a consequence of the plastids degradation observed due to chilling injury (Figure 1 L O). There is a particular case of two spots (Ids 143 and 548 with MW of 67064 and 49456, respectively) identified as transketolases that presented an opposite abundance pattern. Chilled fruits show up-regulation in spot number 143 while spot 548 is down-regulated when compared with control ones (Figure 2A right-side zoom). The lower molecular weight of spot 548 is linked to the fact that the protein sequence coverage is arranged

from the middle up to the end. This could indicate that the referred transketolase has been subjected to degradation. This phenomenon of protein degradation has been previously reported in proteomic studies [51, 52]. Results obtained from tobacco plants with reduced levels of plastidic transketolase suggested that non-allosteric enzymes as transketolase could exert control over carbon fixation, since reductions in transketolase activity had dramatic effects on carbon partitioning between the sucrose and starch biosynthetic pathways [53]. This finding, together with the down-regulation found in PGM, supports the hypothesis that cells are readjusting their metabolism in response to cold stress in order to maintain the level of sugars.

SUPPLEMENTARY DATA

Table S1. Antioxidant enzyme activities (CAT and POX) of bell pepper fruits at harvest day and at the end of both storage treatments (21 days at 1 or 10 ºC with a posterior reconditioning step at 20 ºC in both cases).

Table S2. A comparison of differentially expressed proteins detected in proteomics studies performed in tomato, peach and bell pepper affected by CI

Figure S1. Representative 2D-DIGE images from the Cy5 vs. Cy3 samples gels.

Figure S2. Distribution pattern of proteins from harvest, control and chilled samples in 2D gels.

FUNDING

P.S.B. and I.E. were supported by a postdoctoral position from the JAE-Doc program of National Research Council (CSIC). This work was supported by the Spanish Ministry of Science and Innovation (MICINN) [grants AGL2007-60447 and PIE2009-40I080], and by the Council of Science and Technology from the Region of Murcia (Spain) (Fundación SENECA) [grant 04553/GERM/06].

FIGURE LEGENDS

Figure 1. Visual symptoms of CI and transmission electron microscopy images.

Visual aspect of fruits at harvest (A0) and after 21 days of storage at 10 ºC (A1) or 1 ºC (A2) plus 3 days of reconditioning at 20 ºC. Transmission electron microscopy images from transversal sections of pericarp of *Capsicum annunn*. (A, D, G, J and M) pepper fruits at harvest time, (B, E, H, K and N) pepper fruits after 21 days of storage at 10 ºC (control) plus 3 days of reconditioning at 20 ºC. (C, F, I, L and O) pepper fruits after 21 days of storage at 1 ºC (chilled) plus 3 days of reconditioning at 20 ºC. (A, B and C). Ultrastructure of epidermal cells (Arrows in C show collapsed cytoplasm). (D, E and F) Ultrastructure of Collenchymatic cells under the epidermis (Arrows in F show collapsed cytoplasm). (G, H and I) Mesocarp cells. (J) Detail of a collechymatic cell in control pepper fruit showing a plastid. (K) Detail of a collechymatic cell in control samples (10ºC) showing an altered plastid. (L) Detail of a collechymatic cell in chilled samples (1ºC) showing a degraded cytoplasm and plastid. (M) Detail of a mesocarp cell in day 0 pepper fruit showing a cytoplasm rich in plastids containing starch grains, peroxisomes and mitochondria. (N) Detail of a mesocarp cell in control samples (10ºC) showing a cytoplasm containing altered plastids. (O) Detail of a mesocarp cell in chilled samples (1ºC) showing a degraded cytoplasm containing altered plastids. Ct= Cuticle; CW= Cell Wall; Ep= Epidermal cell; M= Mitochondria; Pt= Plastid; Px= Peroxisome; S= Starch grain.

Figure 2. Proteomic analysis in bell pepper fruits.

(A) Master gel stained with CCB showing protein spots with significant variations. Green colour marks correspond to those spots with significant variation at $p<0.05$, those spots with significant variation at $p<0.01$ are marked with orange colour. Right-side zoom: Details of spots 143 and 548. (B) PCA of the 147 spots that showed significant changes at level $p<0.05$; each dot represents the spot map of a single sample. Four biological replicates (represented with the same colour) were visualized for each sample. The two principal components PC1 and PC2 accounted for 52.3% and 30% of the total variance respectively. (C) Summary of the number of spots obtained in each proteomic analysis step.

Figure 3. Functional classification of protein spots.

(A) Functional classification according to putative function using MapMan software (http://mapman.mpimp-golm.mpg.de/). (B) Different protein patterns created from data on the basis of the protein abundance profiles for control and chilled samples compared with harvest samples, and chilled samples compared with control samples. Up = up-regulation, Down = down-regulation

Figure 4. Ascorbate-glutathione cycle.

Proteins and metabolites down-regulated are indicated with downwards arrows, upwards arrows indicate the proteins that are up-regulated. AA, ascorbic acid; APX, ascorbate-peroxidase; MDHAR, monodehydroascorbate reductase; DHAR, dehydroascorbate reductase; GR, glutathione reductase.

REFERENCES

1. Materska M, Perucka I. Antioxidant activity of the main phenolic compounds isolated from hot pepper fruit (*Capsicum annuum* L.). J Agric Food Chem 2005; 53:1750-1756.
2. Kelletat A, Kader AA. Postharvest technology of horticultural crops (3erd ed.). Oakland, Calif.: University of California, Division of Agriculture and Natural Resources, 2002.
3. Gonzalez-Aguilar G, Gayosso L, Cruz R, Fortiz J, Baez R, Wang C. Polyamines induced by hot water treatments reduce chilling injury and decay in pepper fruit. Post Biol Tech 2000; 18: 19-26.
4. Sevillano L, Sanchez-Ballesta MT, Romojaro F, Flores FB. Physiological, hormonal and molecular mechanisms regulating chilling injury in horticultural species. Postharvest technologies applied to reduce its impact. J Sci Food Agric, 2009; 89: 555-573.
5. Zhang C, Tian S. Crucial contribution of membrane lipids' unsaturation to acquisition of chilling-tolerance in peach fruit stored at 0 degrees C. Food Chem, 2009; 115: 405-411.
6. Hodges DM, Lester GE, Munro KD, Toivonen PMA. Oxidative stress: Importance for postharvest quality. Hortsci, 2004; 39: 924-929.
7. Malacrida C, Valle EM, Boggio SB. Postharvest chilling induces oxidative stress response in the dwarf tomato cultivar Micro-Tom. Physiol Plantarum, 2006; 127: 10-18.
8. Ruelland E, Vaultier M-N, Zachowski A, Hurry V. Cold Signalling and Cold Acclimation in Plants. Adv Bot Res, 2009; 49: 35-150.
9. Hwang E, Kim K, Park S, Jeong M, Byun M, Kwon H. Expression profiles of hot

pepper (*Capsicum annuum*) genes under cold stress conditions. J Biosciences, 2005; 30: 657-667.

10. Baginsky S, Hennig L, Zimmermann P, Gruissem W. Gene Expression Analysis, Proteomics, and Network Discovery. Plant Physiol, 2010; 152: 402-410.
11. Palma JM, Corpas FJ, del Rio LA. Proteomics as an approach to the understanding of the molecular physiology of fruit development and ripening. J Proteomics, 2011; 74: 1230-1243.
12. Lara MV, Borsani J, Budde CO, Lauxmann MA, Lombardo VA, Murray R, Andreo CS, Drincovich MF. Biochemical and proteomic analysis of 'Dixiland' peach fruit (*Prunus persica*) upon heat treatment. J Exp Bot, 2009; 60: 4315-4333.
13. Zhang C, Ding Z, Xu X, Wang Q, Qin G, Tian S. Crucial roles of membrane stability and its related proteins in the tolerance of peach fruit to chilling injury. Amino Acids, 2010; 39: 181-194.
14. Dagar A, Friedman H, Lurie S. Thaumatin-like proteins and their possible role in protection against chilling injury in peach fruit. Post Biol Tech, 2010; 57: 77-85.
15. Nilo R, Saffie C, Lilley K, Baeza-Yates R, Cambiazo V, Campos-Vargas R, Gonzalez M, Meisel LA, Retamales J, Silva H, Orellana A. Proteomic analysis of peach fruit mesocarp softening and chilling injury using difference gel electrophoresis (DIGE). BMC Genomics, 2010; 11:43.
16. Page, D, Gouble, B, Valot, B, Bouchet, JP, Callot, C, Kretzschmar, A, Causse, M, Renard, CMCG, Faurobert, M. Protective proteins are differenttially expressed in tomato genotypes differing for their tolerance to low-temperature storage. Planta. 2010 ; 232: 483–500.
17. Vega-Garcia MO, Lopez-Espinoza G, Chavez Ontiveros J, Caro-Corrales JJ, Delgado Vargas F, Lopez-Valenzuela JA. Changes in Protein Expression

Associated with Chilling Injury in Tomato Fruit. JASHS, 2010; 135: 83-89.

18. Sanchez-Bel P, Egea I, Sanchez-Ballesta MT, Sevillano L, del Carmen Bolarin M, Flores FB. Proteome Changes in Tomato Fruits Prior to Visible Symptoms of Chilling Injury are Linked to Defensive Mechanisms, Uncoupling of Photosynthetic Processes and Protein Degradation Machinery. PCP, 2012; 53: 470-484.
19. Candan A, Graell J, Larrigaudiere C. Roles of climacteric ethylene in the development of chilling injury in plums. Post Biol Tech, 2008; 47: 107-112.
20. Fernandez-Garcia N, Lopez-Perez L, Hernandez M, Olmos E. Role of phi cells and the endodermis under salt stress in Brassica oleracea. New Phytol, 2009; 181: 347-60.
21. Egea MI, Martinez-Madrid MC, Sanchez-Bel P, Murcia MA, Romojaro F. The influence of electron-beam ionization on ethylene metabolism and quality parameters in apricot (Prunus armeniaca L, cv Bulida). Lwt-Food Sci Tech, 2007; 40: 1027-1035.
22. Martinez-Solano J, Sanchez-Bel P, Egea I, Olmos E, Hellin E, Romojaro F. Electron beam ionization induced oxidative enzymatic activities in pepper (*Capsicum annuum* L.), associated with ultrastructure cellular damages. J Agric Food Chem, 2005; 53: 8593-8599.
23. Sanchez-Bel, P, Egea, I, Romojaro, F, Martıinez-Madrid, MC. Sensorial and chemical quality of electron beam irradiated almonds (*Prunus amygdalus*). LWT-Food Sci. Technol. 2008; 41: 442–449.
24. Lowry O, Rosebrough N, Farr A, Randall R. Protein measurement with the folin phenol reagent. J Biol Chem, 1951; 193: 265-275.
25. Havlis J, Thomas H, Sebela M, Shevchenko A. Fast-response proteomics by

accelerated in-gel digestion of proteins. Analytical Chem, 2003; 75: 1300-1306.

26. Altschul SF, Gish W, Miller W, Myers EW, Lipman DJ. Basic local alignment search tool. J Mol Biol, 1990; 215(3): 403-10.
27. Yang J, Fu MR, Zhao YY, Mao LC. Reduction of chilling injury and ultrastructural damage in cherry tomato fruits after hot water treatment. Agric Sci China, 2009; 8(3): 304-310
28. Lim C, Kang S, Cho J, Gross K, Woolf A. Bell pepper (*Capsicum annuum* L.) fruits are susceptible to chilling injury at the breaker stage of ripeness. Hortsci, 2007; 42: 1659-1664.
29. Lim C, Kang S, Cho J, Gross K. Antioxidizing Enzyme Activities in Chilling-sensitive and Chilling-tolerant Pepper Fruit as Affected by Stage of Ripeness and Storage Temperature. JASHS, 2009; 134: 156-163.
30. Candan A, Graell J, Larrigaudiere C. Postharvest quality and chilling injury of plums: benefits of 1-methylcyclopropene. Spanish J Agric Res, 2011; 9: 554-564.
31. Mateos RM, Leon AM, Sandalio LM, Gomez M, Rio LA, Palma JM. Peroxisomes from pepper fruits (*Capsicum annum* L.): purification, characterisation and antioxidant activity. Plant Physiol, 2003; 160: 1507-1516.
32. Rogiers S, Kumar G, Knowles N. Maturation and ripening of fruit of Amelanchier alnifolia Nutt. are accompanied by increasing oxidative stress. Annals of Botany, 1998; 81: 203-211.
33. Tripathi B, Bhatt I, Dietz K. Peroxiredoxins: a less studied component of hydrogen peroxide detoxification in photosynthetic organisms. Protoplasma, 2009; 235: 3-15.
34. Miyake C, Asada K. Thylakoid bound ascorbate peroxidase in spinach chloroplasts and photoreduction of its primary oxidation product monodehydroascorbate radicals in thylakoids. PCP, 1992; 33: 541-553.

35. Eltelib H, Badejo A, Fujikawa Y, Esaka M. Gene expression of monodehydroascorbate reductase and dehydroascorbate reductase during fruit ripening and in response to environmental stresses in acerola (Malpighia glabra). J Plant Physiol, 2011; 168: 619-627.
36. Strand A, Foyer CH, Gustafsson P, Gardestrom P, Hurry V. Altering flux through the sucrose biosynthesis pathway in transgenic Arabidopsis thaliana modifies photosynthetic acclimation at low temperatures and the development of freezing tolerance. Plant Cell Env, 2003; 26: 523-535.
37. Danyluk J, Perron A, Houde M, Limin A, Fowler B, Benhamou N, Sarhan F. Accumulation of an acidic dehydrin in the vicinity of the plasma membrane during cold acclimation of wheat. Plant Cell, 1998; 10: 623-638.
38. Wen FP, Zhang ZH, Bai T, Xu Q, Pan YH. Proteomics reveals the effects of gibberellic acid (GA(3)) on salt-stressed rice (Oryza sativa L.) shoots. Plant Sci, 2010; 178: 170-175.
39. Seki M, Narusaka M, Abe H, Kasuga M, Yamaguchi-Shinozaki K, Carninci P, Hayashizaki Y, Shinozaki K. Monitoring the expression pattern of 1300 Arabidopsis genes under drought and cold stresses by using a full-length cDNA microarray. Plant Cell, 2001; 13: 61-72.
40. Bae MS, Cho EJ, Choi EY, Park OK. Analysis of the Arabidopsis nuclear proteome and its response to cold stress. Plant Journal, 2003; 36: 652-663.
41. Holtgrefe S, Gohlke J, Starmann J, Druce S, Klocke S, Altmann B, Wojtera J, Lindermayr C, Scheibe R. Regulation of plant cytosolic glyceraldehyde 3-phosphate dehydrogenase isoforms by thiol modifications. Physiol Plantarum, 2008; 133: 211-228.
42. Hameister S, Becker B, Holtgrefe S, Strodtkoetter I, Linke V, Backhausen JE,

Scheibe R. Transcriptional regulation of NADP-dependent malate dehydrogenase: Comparative genetics and identification of DNA-binding proteins. J Molecular Evolution, 2007; 65: 437-455.

43. Yao YX, Dong QL, Zhai H, You CX, Hao YJ. The functions of an apple cytosolic malate dehydrogenase gene in growth and tolerance to cold and salt stresses. Plant Physiol Biochem, 2011; 49: 257-264.
44. Noguchi K, Yoshida K. Interaction between photosynthesis and respiration in illuminated leaves. Mitochondrion, 2008; 8: 87-99.
45. Pastore D, Trono D, Laus M, Di Fonzo N, Flagella Z. Possible plant mitochondria involvement in cell adaptation to drought stress - A case study: durum wheat mitochondria. J Exp Bot, 2007; 58: 195-210.
46. Givan, CV. Aminotransferases in higher plants. In: Stumpf PK, Conn EE (eds) The biochemistry of plants. Academic Press, New York, 1980, p.329-357
47. Parys E, Jastrzebski H. Light-enhanced dark respiration in leaves, isolated cells and protoplasts of various types of C-4 plants. J Plant Physiol, 2006; 163: 638-647.
48. Coruzzi G, Bush D. Nitrogen and carbon nutrient and metabolite signaling in plants. Plant Physiol, 2001; 125: 61-64.
49. Fernie AR, Carrari F, Sweetlove LJ. Respiratory metabolism: glycolysis, the TCA cycle and mitochondrial electron transport. Current Opinion in Plant Biology, 2004; 7: 254-261.
50. Airaki M, Leterrier M, Mateos RM, Valderrama R, Chaki M, Barroso JB, Del Río LA, Palma JM, Corpas FJ. Metabolism of reactive oxygen species and reactive nitrogen species in pepper (*Capsicum annuum* L.) plants under low temperature stress. Plant Cell Env, 2012; 35: 281-295.
51. Dani V, Simon W, Duranti M, Croy R. Changes in the tobacco leaf apoplast

proteome in response to salt stress. Proteomics, 2005; 5: 737-745.

52. Razavizadeh R, Ehsanpour A, Ahsan N, Komatsu S. Proteome analysis of tobacco leaves under salt stress. Peptides, 2009; 30, 1651-1659.

53. Henkes S, Sonnewald U, Badur R, Flachmann R, Stitt M. A small decrease of plastid transketolase activity in antisense tobacco transformants has dramatic effects on photosynthesis and phenylpropanoid metabolism. Plant Cell, 2001; 13: 535-551.

54. Paul M, Pellny T. Carbon metabolite feedback regulation of leaf photosynthesis and development. J Exp Bot, 2003; 54: 539-547

Table

Click here to download Table: Table 1.docx

Table 1**.** Physiological parameters and metabolite contents in fruits after 21 days of storage at 10 ºC (control) or 1 ºC (chilled) plus 3 days of reconditioning at 20 ºC.

	Control	Chilled
Ethylene (nL g^{-1} h^{-1}**)**	0.75 ± 0.015 a	5.07 ± 1.15 b
Lipid peroxidation (nmol MDA g^{-1} h^{-1})	99.45 ± 3.80 a	117.20 ± 3.01 b
Sucrose (mg 100g FW^{-1})	0.16 ± 0.01 b	0.32 ± 0.03 a
Glucose (mg 100g FW^{-1})	2.42 ± 0.25 a	2.13 ± 0.17 a
Fructose (mg 100g FW^{-1})	2.28 ± 0.13 b	2.82 ± 0.24 a
Oxalic acid (mg 100g FW^{-1})	2.86 ± 0.22 a	1.95 ± 0.23 b
Citric acid (mg 100g FW^{-1})	2.90 ± 0.15 a	1.26 ± 0.17 b
Malic acid (mg 100g FW^{-1})	nd	1.73 ± 0.67
Succinic acid (mg 100g FW^{-1})	7.02 ± 1.07 b	9.66 ± 4.69 a
Ascorbic acid (mg 100g FW^{-1})	196.11 ± 11.82 a	120.55 ± 2.73 b

Values represent the means ± SD of four replicates (3 fruits each).

Means within a parameter without a common letter are significantly different by t-test ($p< 0.05$).

nd. Non-detected

Table

Click here to download Table: Table 2.docx

Table 2. Identified protein spots, functional classification and their accumulation (fold change).

Pattern	Spot no[a].	Assignment[b]	UniProt accesion no.	% Coverage	Matched/ Unmatched[c] (Score)[d]	MS/MS ions[e] (score)	TargetP[h]	Species	Nominal Mr	Calculated Mr	Nominal pI	Fold Change[f] C/H	Ch/H	Ch/C
Amino acid metabolism														
E	38	Methionine synthase	Q42699	9	8/38(90)	YLFAGVVDGR (21)	C	*Catharanthus roseus*	74498	84857	6.1	1.07	-1.89	-2.02
E	80	Methionine synthase	Q42699	21	14/55(241)	GVTGFGFDLVR (18)	–	*Catharanthus roseus*	84857.3	74157	6.1	1.03	-1.95	-2
F	648	Aspartate aminotransferase	P46248	18	11/59(83)	AGITVIQIDEAALR(29)	C	*Arabidopsis thaliana*	49831.3	46571	8.18	1.86	1.03	-1.8
C1-metabolism														
A	671	Formate dehydrogenase	Q07511	25	12/60 (92)	DGELAPQYR(19) YAAGTKDMLDR(19) YAAGTKDMLDR(22)	M	*Solanum tuberosum*	41545.6	45706	6.9	1	1.81	1.81
Cell wall														
F	802	Polygalacturonase inhibitor	D7RJV7	18	20/40(153)	GLGNPYDLITWDPK(73) LDLNHNKIYGSLPTILT K (149)	S	*Capsicum annuum*	38247	36504	8.99	4.11	1.39	-2.97
F	1571	Xyloglucan endotransglucosylase/hydrolase protein	P93046	18	12/43(93)	GSGDGNIIGR (18) VYDYCRDPR (32) VYDYCRDPR (23)	M	*Arabidopsis thaliana*	33540.7	33540	9.03	12.91	3.99	-3.23
Cell organisation														
E	1462	Peptidyl-prolyl cis-trans isomerase	Q9ASS6	14	4/60(73)	IVIGLYGDDVPQTAENF R(59) LIESQETDRGDRPR(1)	M	*Arabidopsis thaliana*	28306.1	28306	9.39	1.86	-1.08	-2

E	930	Annexin cap32	Q9SB88	16	8/57(86)	SNFVLVEIACTR(22) GLVYPEHYFVEVLR(4) SLEEDVAYHTTGDHR(14)	M	*Capsicum annuum*	35858.7	37271	5.85	1.49	-1.14	-1.7
E	938	Annexin cap32	Q9SB88	62	26/39(271)		–	*Capsicum annuum*	35858.7	36203	5.85	2.11	-1.01	-2.12
E	948	Fibrillin	Q42493	23	12/53 (206)	GDAGSIFVLIK(80) QLTDSFYGTNR(37) KQLTDSFYGTNR(15) AEIVELITQLESK(26)	C	*Capsicum annuum*	35260.1	35635	5.08	2.35	-1.58	-3.72
Fermentation														
E	357	Aldehyde dehydrogenase	Q9SU63	24	13/52(77)		M	*Arabidopsis thaliana*	58588.9	55886	7.11	1.68	-1.2	-2.02
E	365	Aldehyde dehydrogenase	Q9SU63	15	18/47(132)	TFQGPPHGIQVER(36)	M	*Arabidopsis thaliana*	58588.9	55886	7.11	2	-1.34	-2.68
E	372	Aldehyde dehydrogenase	Q9SU63	17	13/52(141)	TFPTLDPR(34) YYAGWADK(52)	M	*Arabidopsis thaliana*	58588.9	55502	7.11	2.77	-1.66	-4.58
Glycolysis														
D	717	Fructose-bisphosphate aldolase	P17784	11	5/60(97)	VAPEVIAEYTVR(38)GILAADESTGTIGKR(48)	–	*Oryza sativa*	38863.4	44200	6.96	-1.26	-3	-2.38
E	873	Fructose-bisphosphate aldolase	Q38JH2	30	10/55(74)		–	*Solanum tuberosum*	42327.1	39620	8.19	1.26	-1.8	-2.26
B	409	Enolase	P26300	30	16/49(176)	KAGWGVMTSHR(3) ISGDQLKDLYK(2) AAVPSGASTGIYEALELR(99)	S	*Solanum lycopersicum*	47798.3	54418	5.68	-1.43	1.04	1.5
E	259	Glucose-6-phosphate isomerase	Q1PCD2	1	x	FLANVDPIDVAR(39)	–	*Solanum lycopersicum*	62685.5	59466	6.39	1.57	-1.03	-1.61
E	557	Glyceraldehyde-3-phosphate dehydrogenase	P04796	5	x	GILGYTEDDVVSTDFVGDNR(59)	–	*Sinapsis alba*	36924.3	49310	7.7	1.69	-1.64	-2.78

D	750	Glyceraldehyde-3-phosphate dehydrogenase	Q8VWP1	33	13/52(253)	SSIFDAKAGIALSK(94) AASFNIIPSSTGAAK(88)	–	*Capsicum annuum*	34485.4	43167	6.19	-1.01	-4.52	-4.46
E	754	Glyceraldehyde-3-phosphate dehydrogenase	Q8VWP1	34	13/52(139)	VIHDRFGIVEGLMTTV HSITATQK(22)	–	*Capsicum annuum*	34485.4	43082	6.19	1.02	-4.22	-4.29
D	756	Glyceraldehyde-3-phosphate dehydrogenase	Q8VWP1	17	9/56(173)	SSIFDAKAGIALSK(69)	–	*Capsicum annuum*	34485.4	43209	6.19	-1.34	-2.65	-1.97
E	767	Glyceraldehyde-3-phosphate dehydrogenase	Q8VWP0	12	13/52 (98)	TVDGPSMKDWR(6) TVDGPSMKDWR(8) AASFNIIPSSTGAAK(22) LVSWYDNEWGYSSR(26)	–	*Capsicum annuum*	34171	42997	6.14	1.15	-2.92	-3.35
D	768	Glyceraldehyde-3-phosphate dehydrogenase	Q8VWP1	25	10/55 (195)	TVDGPSMKDWR(10) AASFNIIPSSTGAAK(12) LVSWYDNEWGYSSR(15) GILGFTEDDVVSTDFVG DSR(132)	–	*Capsicum annuum*	34485.4	42158	6.14	-1.01	-2.05	-2.03
E	198	Phosphoglucomutase	Q9M4G4	23	14/51(88)	YLFEDGSR(27) LSGTGSEGATIR(3)	–	*Solanum tuberosum*	63469.8	62841	6.01	1.05	-1.69	-1.79
E	212	Phosphoglucomutase	Q9ZSQ4	2	x	DNLGGDKLVTVEDIVR (77)	–	*Populus tremula*	63123.6	62286	5.49	1.22	-2.55	-3.12
N-metabolism														
E	583	Glutamate dehydrogenase	P93541	7	x	DDGTLASFVGFR(42) GGIGCSPSDLSISELER(55	M	*Solanum lycopersicum*	44813.3	48827	6.68	1.36	-1.77	-2.41
Not assigned.unknown														
E	1060	S-formylglutathione hydrolase	Q8LAS8	16	8/57(79)	MFGGYNKR(1) ELPTLLHENFPELDTSR(57)	–	*Arabidopsis thaliana*	31655.6	33474	5.91	1.18	-1.79	-2.12
Protein degradation														
E	1190	Proteasome subunit alpha type-6	Q9XG77	20	18/47 (144)	AAGITSIGVR(24) YLGLLATGMTADAR(16)	–	*Nicotiana tabacum*	27303.1	29362	5.92	1.78	-1.64	-2.93

PS calvin cycle													
D	834	Fructose-bisphosphate aldolase	G8FMI9	18	8/57(74)	SAAYYQQGAR(22) LASIGLENTEANR(24)	C	*Carica papaya*	42941.8	40210	6.79	-1.06	-2.37	-2.23
D	416	Ribulose bisphosphate carboxylase large chain	Q31951	45	29/46(254)		–	*Capsicum baccatum*	52030.3	54418	6.54	-1.01	-2.14	-2.13
B	143	Transketolase	O78327	46	34/31(294)		C	*Capsicum annuum*	80398	67064	6.16	-1.36	1.12	1.52
E	548	Transketolase	O78327	14	14/51(78)	SIITGELPAGWEK(4) VSIEAGSTFGWEK(2) VSIEAGSTFGWEK(15)	C	*Capsicum annuum*	80398	49456	6.16	3.03	-1.36	-4.11
Redox														
E	1306	Probable glutathione S-transferase	Q03666	10	x	SPLLLQMNPIHK(14) SPLLPSDPYKR(4) FWADYVDKK(4) FWADYVDKK(20)	S	*Nicotiana tabacum*	25788.9	26267	5.67	1.32	-1.3	-1.72
E	822	Probable NADP-dependent oxidoreductase	Q9SLN8	4	x	YFPDGIDIYFENVGGK (53)	–	*Arabidopsis thaliana*	37988.8	40809	8.09	1.22	-2.49	-3.04
C	581	Monodehydroascorbate reductase	Q43497	22	11/54(122)	AYLFPEGAAR(3) EAVAPYERPALSK(29) SVDEYDYLPYFYSR(48)	–	*Solanum lycopersicum*	47035.7	49020	5.77	-1.6	-1.03	1.55
E	1154	L-ascorbate peroxidase	Q42661	42	12/53(86)		–	*Capsicum annuum*	27117.6	30302	5.21	1.42	-2.09	-2.97
E	1298	GSH-dependent dehydroascorbate reductase	Q4VDN8	6	x	LYHLKVALGHFKK (84)	–	*Solanum lycopersicum*	23406.9	26579	5.79	1.01	-1.5	-1.52
D	1299	GSH-dependent dehydroascorbate reductase	Q4VDN8	25	7/58(89)	VPVINFGDK(33) WFLEVNPEGK(4) WFLEVNPEGK(32)	–	*Solanum lycopersicum*	23406.9	26423	5.79	-1.22	-2.8	-2.3
F	230	Catalase	Q9M5L6	22	12/53(78)	CAHHNNHR(9) SHIQENWR(16)	–	*Capsicum annuum*	56480	56479	7.31	5.51	1.4	-3.92

E	362	Catalase	P55311	54	29/36(237)		–	*Solanum melongena*	56620.2	55941	6.86	1.41	-3.14	-4.41
E	366	Catalase	Q9M5L6	39	22/43(161)		–	*Capsicum annuum*	56480	55941	7.31	1.06	-2.27	-2.4
D	371	Catalase	Q9M5L6	17	13/52(141)		–	*Capsicum annuum*	56480	55941	7.31	-1.11	-1.74	-1.57
B	1279	Glutathione S-transferase ERD13	P42761	26	7/58(107)	LFESHAILR(29) TPEYQEVNIMK(12) TPEYQEVNIMK(63) TPEYQEVNIMK(45)	S	*Arabidopsis thaliana*	24230	27028	5.49	-1.74	1.06	1.84
B	1333	Superoxide dismutase	O49066	10	6/59(98)	LVIETTANQDPLVIK(67) LVIETTANQDPLVIK(37) RLVIETTANQDPLVIK(5) RLVIETTANQDPLVIK(15)	M	*Capsicum annuum*	25512.2	24979	8.39	-1.34	1.41	1.89
B	1439	Thioredoxin peroxidase	Q8SAG2	16	8/57(82)	GDAGSIFVLIK(6)QLTDSFYGTNR(40)QLTDSFYGTNR(22)	–	*Capsicum annuum*	17406.1	17427	5.17	-1.57	1.42	2.24
RNA processing														
E	551	Maturase K (Intron maturase)	B1NWD1	43	11/54(76)		M	*Manihot esculenta*	60615.7	49262	9.6	1.67	-2.24	-3.74
Secondary metabolism														
E	423	Capsanthin/capsorubin synthase	Q42435	4	x	DSHLGNEPYLR(21) LFDAFFDVDPK(38)	C	*Capsicum annuum*	56658.7	53831	8.77	4.22	-1.29	-5.43
Stress														
A	961	Glucan endo-1,3-beta-glucosidase, acidic isoform	P36401.1	x[g]	x[g]	LEYALFTSNPVVLTNDGR	S		36994.7	36185	5.21	9.47	15.4	1.63
A	1415	Pathogenesis-related protein PR10	Q9M500	44	13/52(89)	GAYTFTDKSTASVAPSR(89) ALVIDFNNLVSK(78) ALVIDFNNLVSKLAPDV(58)	–	*Capsicum annuum*	17390	17294	5.66	1.62	14.85	9.14

A	1426	Pathogenesis-related protein PR10	Q9M500	47	14/51(101)		_	*Capsicum annuum*	17390	20672	5.66	1.64	16.08	9.82
Tricarboxilic Cycle Acid. TCA.														
E	748	Malate dehydrogenase, cytoplasmic	O48905	30	11/54(257)	EFAPSIPEKNITCLTR(84) EFAPSIPEKNITCLTR(95) NGEWSIVQGLPIDEFSR(116)	-	*Medicago sativa*	35546.9	43252	6.39	1.12	-2.07	-2.31
E	758	Malate dehydrogenase, cytoplasmic	O48905	33	11/54(216)	VLVTGAAGQIGYALVPMIAR(66) EFAPSIPEKNITCLTR(94)	-	*Medicago sativa*	35546.9	42912	6.39	1.31	-1.61	-2.11
E	538	Citrate synthase	O80433	28	14/51(93)	HAFGDQY(20) TIEAEAAHGTVTR(8)	M	*Daucus carota*	52656.6	50690	6.95	1.64	-1.44	-2.37
F	582	Isocitrate dehydrogenase	P50218	32	12/53(82)		_	*Nicotiana tabacum*	46729.3	49020	6.06	1.95	1.13	-1.72
transport.p- and v-ATPases														
E	1078	V-type proton ATPase	Q9SWE7	32	10/55(81)	IRQEYER(4) IVCENTLDAR(32) IVCENTLDAR(11)	_	*Citrus limon*	26343.3	32821	7.13	2.94	-1.66	-4.89

[a] Spot number as assigned in gel master
[b] Protein assignment based on LC-MS/MS identification
[c] Number of peptides matched/unmatched in MS analysis. Proteins identified by MS/MS are designed with x.
[d] Mascot score (S=−10*Log(P)); where P is the probability that the observed match is a random event. In all cases, the probability score was <0.05.
[e] Amino acid sequence identified by MS/MS when protein identification was performed by combined search (peptide mass fingerprint plus MS/MS); the ion score is indicated in parentheses.
[f] Values reported indicate the protein accumulation pattern (fold change) between the conditions shown above them. C = control samples, Ch = chilled samples, H= harvest day samples
[g] identification made by *de novo* sequencing and a search by sequence homology. Positive identities found = 14/18 (77%)
[h] subcellular localization predicted by TargetP:

C Chloroplast, i.e. the sequence contains **cTP**, a chloroplast transit peptide;
M Mitochondrion, i.e. the sequence contains **mTP**, a mitochondrial targeting peptide;
S Secretory pathway, i.e. the sequence contains **SP**, a signal peptide;
_ Any other location;

Figure

Click here to download Figure: Figure 1.pptx

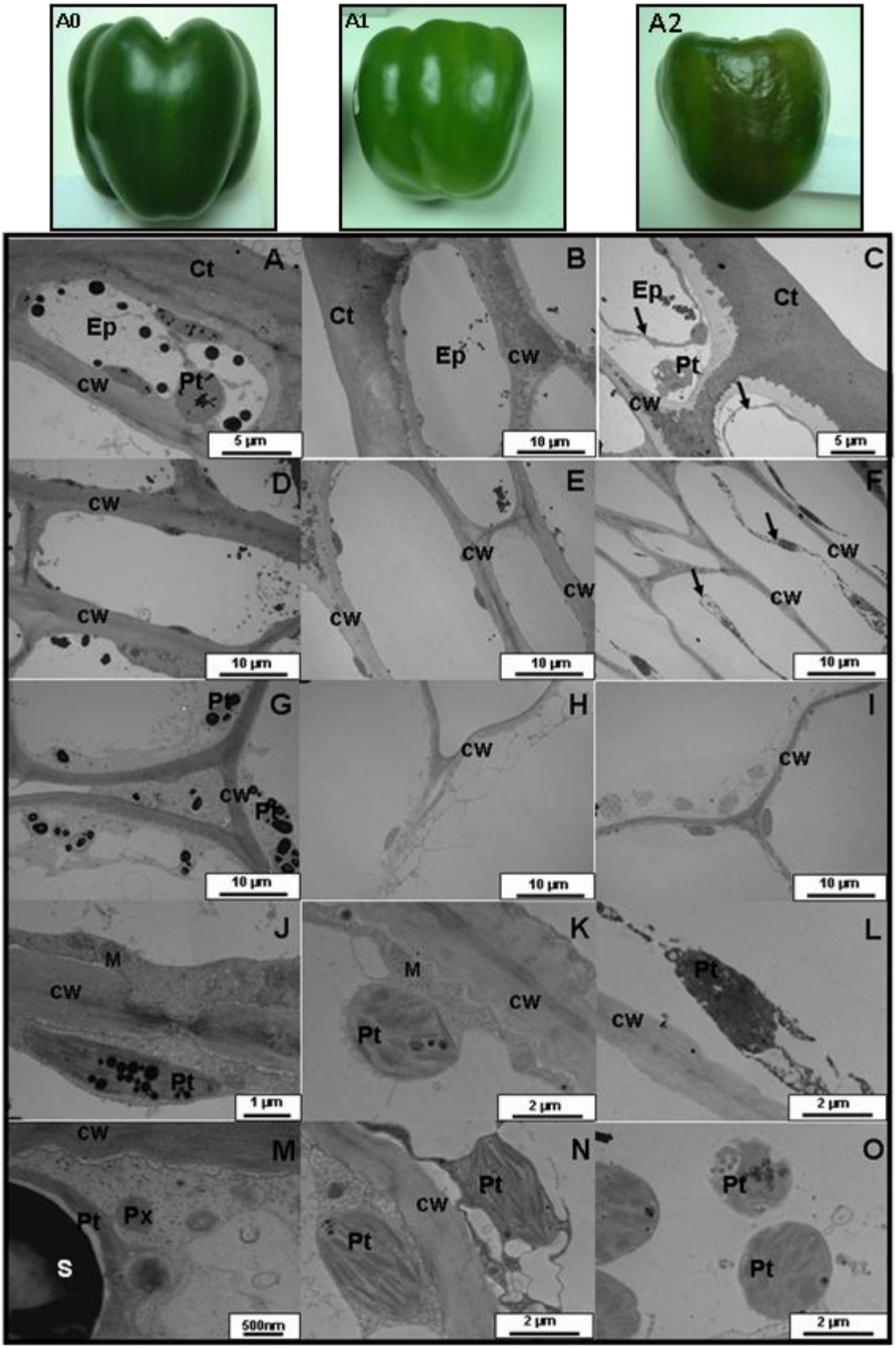

Figure

Click here to download Figure: Figure 2.pptx

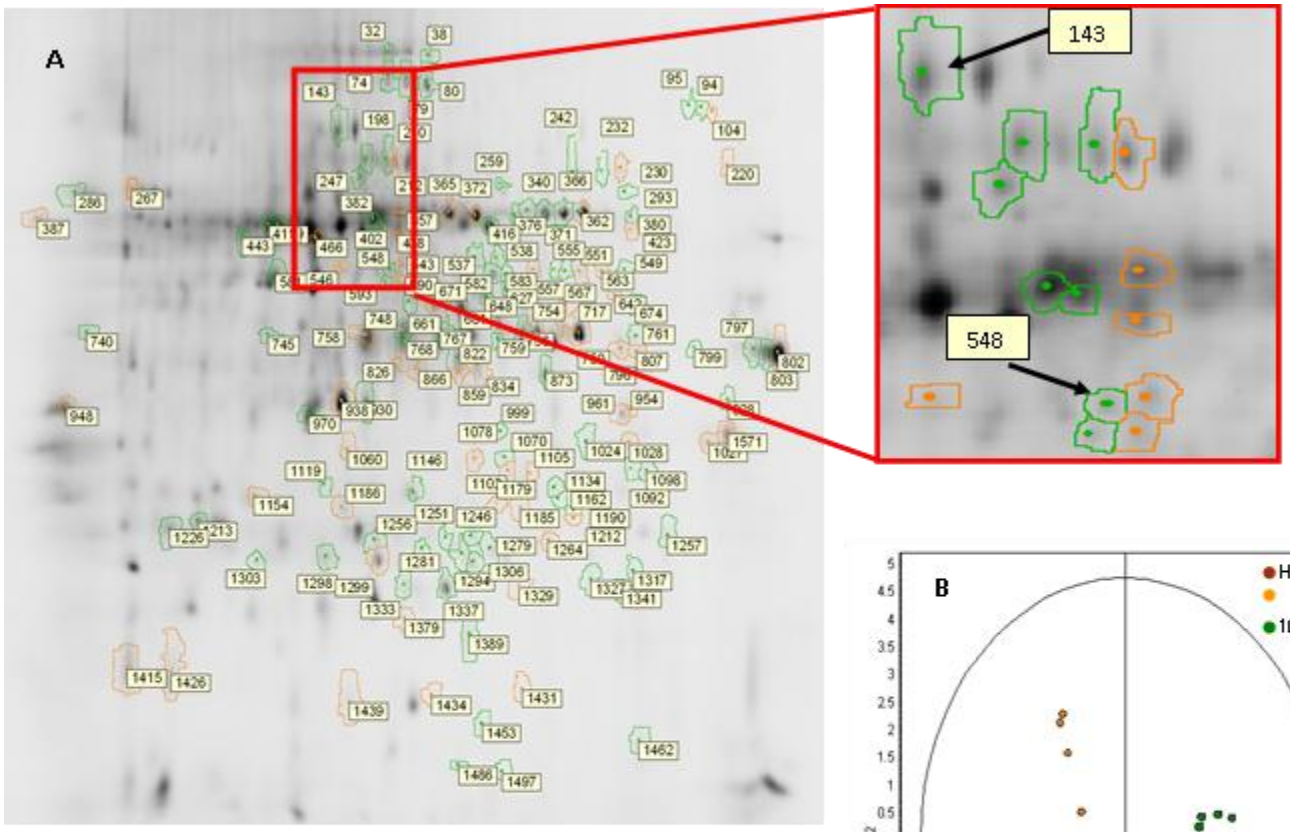

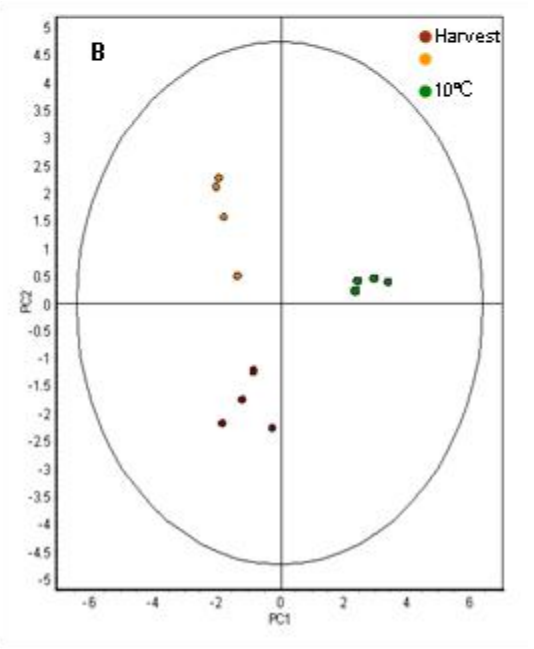

C	Total	Up-regulated	Down-regulated
Spots with significant variation in their expression	147	41	106
Spots identified by MS/MS	67	15	52
Spots with Fold Change >1.5	55	10	45

Figure

Click here to download Figure: Figure 3.pptx

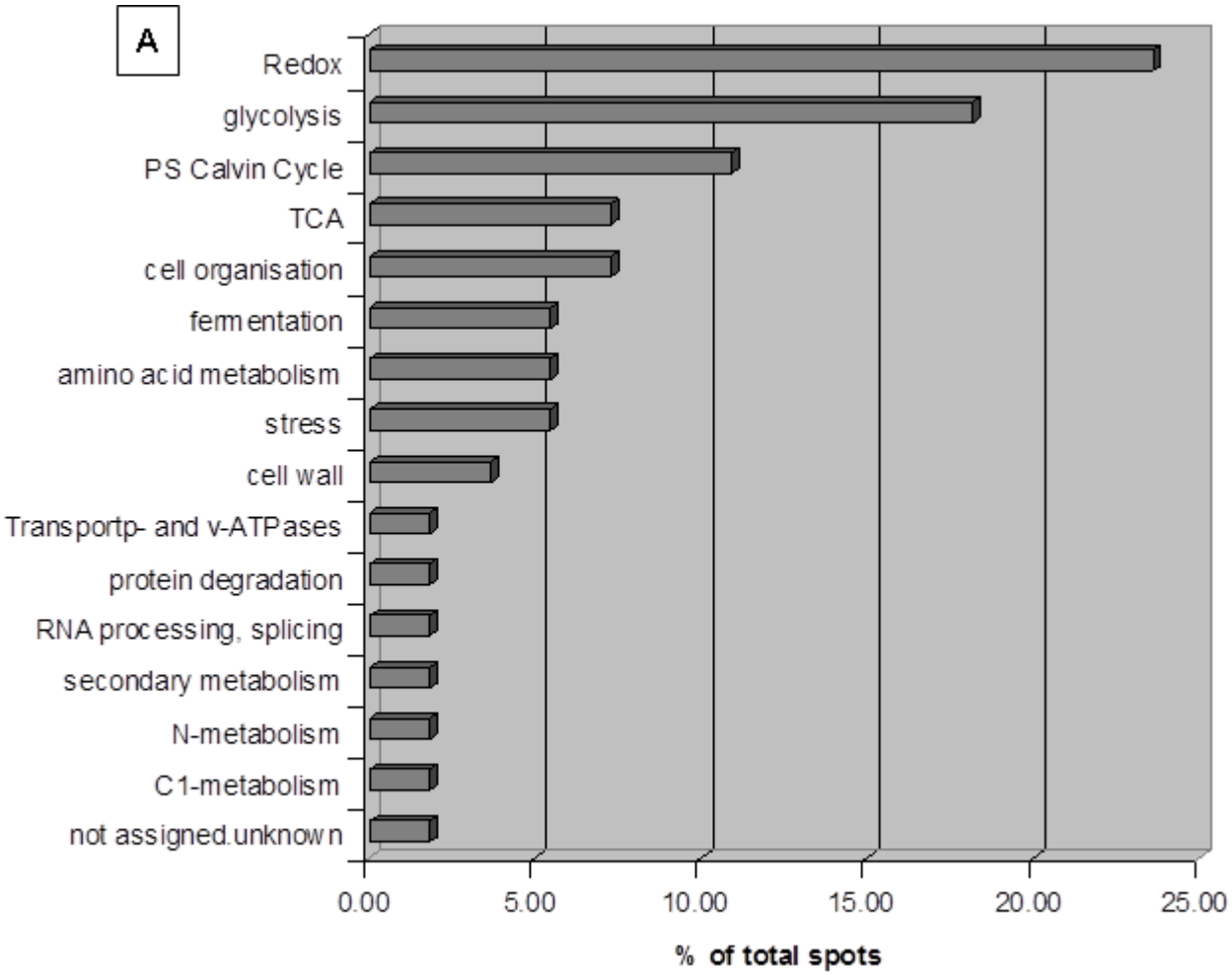

B

Pattern	Expression profiles		
	Control/day 0	Chilled/day 0	Chilled/Control
A	Up	Up	Up
B	Down	Up	Up
C	Down	Down	Up
D	Down	Down	Down
E	Up	Down	Down
F	Up	Up	Down

Figure

Click here to download Figure: Figure 4.pptx

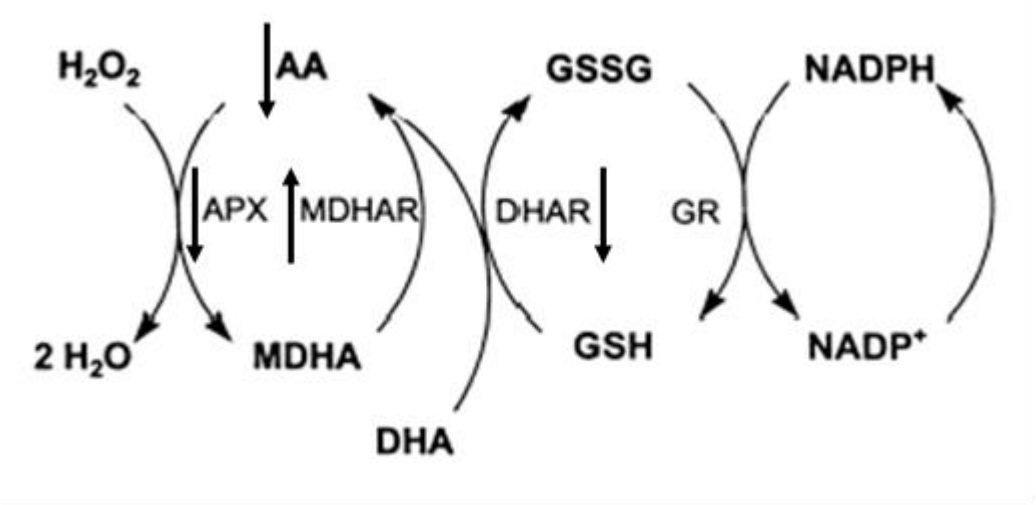

Supplementary material

Click here to download Supplementary material: Supplementary table 1.doc

Supplementary material

Click here to download Supplementary material: Supplementary table S2.xls

Supplementary material

Click here to download Supplementary material: Supplementary figures.doc